Throughput and delay analysis of cognitive M2M communications

Soumen Mondal [a], Luca Davoli [b,*], Sanjay Dhar Roy [a], Sumit Kundu [a], Gianluigi Ferrari [b], Riccardo Raheli [b]

[a] *Department of Electronics and Communication Engineering, National Institute of Technology, Durgapur, India*
[b] *Department of Engineering and Architecture, University of Parma, Parma, 43124, Italy*

ARTICLE INFO

ABSTRACT

In this paper, we analyze throughput and delay performance of clustered Machine Type Communication (MTC) devices which access an eNodeB utilizing a primary spectrum in underlay mode. We assume that the MTC devices form two clusters and there is an optimal preamble allocation between the two clusters to maximize the throughput. We further investigate the impact of the tolerable interference threshold on throughput, successful preamble decoding probability, and delay. Then, the impact of the preamble partition factor and the access barring factor on throughput and delay is analyzed. Finally, we evaluate the impact of the number of devices, retransmission requests, and preamble partitions on the delay.

1. Introduction

Machine-to-Machine (M2M) communication is evolving as a promising paradigm in emerging 5G networks, which will support Internet of Things (IoT). IoT has gained phenomenal momentum due to significant commercial and research interest. Furthermore, Narrow-Band IoT (NB-IoT) has been standardized under the Third Generation Partnership Project (3GPP) to provide reliable connections among large numbers of inexpensive low power IoT devices over large areas (Ha et al., 2018). M2M communications represent an enabling technology for IoT networking, as they differ from Human-to-Human (H2H) communications in several distinct features, such as: small amount of data transmission; sporadic data transmission; delay; tolerance; and group-based operations (3GPP, 2011). In this scenario, a substantial number of IoT devices will face a shortage of available spectrum. Cognitive Radio (CR) has emerged as a potential approach to solve the conflicting problems of shortage and under-utilization of the available spectrum. It allows unlicensed secondary users to access the spectrum allocated to licensed users or Primary Users (PUs) either opportunistically (in the absence of PUs) or without creating unacceptable interference to existing PUs (if the presence of PUs) (Mitola and Maguire, 1999).

CR-enabled IoT devices will be able to optimize spectrum utilization through spectrum sensing and dynamic spectrum access capabilities (Aijaz and Aghvami, 2015). The throughput performance of M2M communications is evaluated in Lee et al. (2011), where two different approaches for dividing the available Random Access (RA) preambles are considered using an Access Class Barring (ACB) mechanism

(Di et al., 2019). A dynamic, delay-tolerant, and delay-sensitive scheme for the allocation of Random Access CHannel (RACH) resources between two clusters of devices is proposed in Li et al. (2015). The proposed scheme is shown to improve access probability and reduce access delay. While Machine Learning (ML)-based RA schemes have gathered considerable attention in recent years (Zhang et al., 2023, 2022), the optimization of access delay in these schemes continues to be a challenge. In Jiang et al. (2018), repeated preamble retransmissions in the presence of collisions are considered in the RACH procedure and the RACH success probability is evaluated, in the end demonstrating how the utilization of a repetition scheme has been shown to notably enhance the RACH success probability. The authors in Guo et al. (2022) propose a collision-aware ACB RA scheme that incorporates dynamic adjustments to both the ACB factor and preamble resources. In Chowdhury and De (2022), the authors have presented an approach that involves dynamically assigning higher priority in ACB to Machine Types Devices (MTDs) whose data queue sizes approach their buffer limits. To mitigate contention during preamble access, in Swain and Subudhi (2023) Deep Learning (DL)-based models have been adopted to design a RACH procedure. This approach aims at predicting incoming connection requests in advance, and allowing for proactive allocation of uplink resources to UEs.

A transmission scheme for low volume data is proposed in Oh and Shin (2017), in the context of 3GPP NB-IoT networks avoiding a Radio Resource Control (RRC) set up (Debbabi et al., 2022): the access success probability and uplink utilization are shown to improve significantly.

However, no cognitive scenario is considered in Oh and Shin (2017). A cognitive cellular system architecture for M2M communications, along with possible transmission scenarios, is presented in Ejaz and Ibnkahla (2015), where energy-efficient resource allocation is also considered.

An advanced power allocation policy in a CR-based M2M network, where multiple unlicensed M2M devices share the same licensed spectrum of a PU, is investigated in Yao et al. (2014). Underlay CR enabling Machine Type Communication (MTC) devices sharing the spectrum of PUs, such as cellular UE, is studied in Alhussien and Gulliver (2022), where power allocation problems are addressed for improving the energy efficiency of MTC devices by minimizing their power consumption or maximizing their energy efficiency. A cognitive clustered M2M communication with a joint selection of cellular equipment and M2M devices is analyzed in Abdullah et al. (2019) to reduce outage of M2M. A hybrid duplex Base Station (BS) switching between half-duplex and full-duplex modes to attain the best performance is considered.

In Li et al. (2018), the throughput of a RA narrowband CR IoT network is maximized through selection of optimal sensing parameter via collaborative sensing. In detail, the trade-off between RA NB-CR-IoT network throughput and sensing accuracy is investigated, and a set of optimal (throughput maximizing) sensing parameter is derived. Throughput and delay performance of massive multi-group RA M2M communication in industrial IoT (IIoT) is studied in Zhang et al. (2019). MTDs are divided into multiple groups on the basis of their delay requirement, and a double queue model is used to characterize the access behavior of each MTD device. To this end, throughput of delay tolerant MTDs is maximized under delay constraints of delay-sensitive MTDs by an appropriately tuning back-off parameters of delay-sensitive MTDs.

Given the scarcity in spectrum due to the exponential growth of the number of MTC devices, the licensed spectrum of a PU needs to be utilized in cognitive mode. In the process of accessing the primary spectrum in underlay mode, the analysis of throughput and delay of MTC devices, as a performance metrics, is important while satisfying the Quality of Service (QoS) of the PU. MTC devices may occur in cluster or groups and may be controlled by secondary BSs or eNBs of that group. However, while the above-discussed literature on cognitive M2M communications considers several aspects of M2M communications in cognitive mode, to the best of our knowledge, a comprehensive analysis of throughput and delay of a cluster of MTC devices, with an appropriate division of RA preambles while satisfying QoS of licensed PU in terms of an outage constraint in underlay cognitive mode, is missing. Furthermore, the impact of tolerable interference in an underlay mode on the performance of cluster-based MTC devices and appropriate division of RA preambles need to be investigated.

Given the "gaps" highlighted in the above literature works and compared, for the sake of completeness, in Table 1, in this paper the performance of cellular-based IoT devices coexisting with a primary network in an underlay mode is examined. In particular, two clusters of IoT devices, which share the frequency band of a transmitter–receiver pair of PUs in an underlay mode while communicating to their corresponding eNB, are considered. We evaluate the successful decoding probability of a MTC device belonging to a cluster and satisfying a cognitive constraint (i.e., the interference at the PU receiver is kept below a tolerable threshold). Partitioning of RACH preambles between two clusters is considered in order to maximize the throughput. An analytical expression for the optimal number of preambles to be allocated to each cluster to maximize the throughput is derived. To the best of our knowledge, the investigation of a transmission scheme of two clusters of IoT devices sharing a common spectrum of a transmitter–receiver pair of PUs in an underlay mode and the analysis of throughput and delay performance for such networks are novel.

Overall, the major contributions of our paper can be highlighted as follows.

- We propose a novel network model with two clusters of MTC devices accessing the licensed spectrum of a PU.
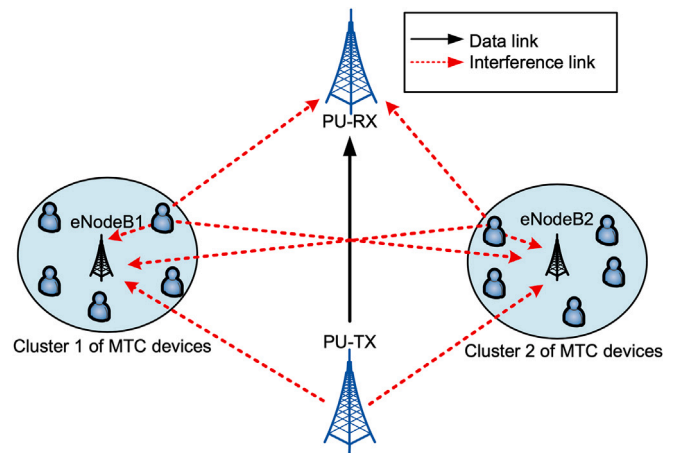

Fig. 1. System model composed by two clusters of MTC devices co-existing with a transmitter–receiver pair of PUs.

- We evaluate the throughput and delay performance of two clusters of MTC devices.
- We develop a novel analytical framework to evaluate the successful decoding probability of MTC devices of two clusters (as shown in Fig. 1) at their associated eNBs, with all the devices sharing the frequency band of a transmitter–receiver pair of PUs in underlay mode.
- We derive a novel analytical expression for optimal RA preamble partition (Yang et al., 2023) between the two clusters, in order to maximize the throughput.
- We derive the impact of the tolerable interference threshold at the PU receiver and the portion of tolerable interference allowed by each cluster on the decoding probability and throughput. Furthermore, we evaluate the impacts of the primary outage constraint, the ACB mechanism, and the number of preambles on the throughput and delay.
- We develop a MATLAB-based simulation framework in order to validate the results predicted by our novel analytical framework.

The remainder of this paper is organized as follows. The proposed communication system model is introduced in Section 2. The performance evaluation is carried out in Section 3. In Section 4, simulation results are presented and discussed. Finally, in Section 5 we draw our conclusions.

2. System model

We consider two eNBs with two clusters of IoT devices that co-exist with a transmitter–receiver pair of PUs. In cluster #1, MTC devices access eNodeB1 whereas in cluster #2 MTC devices access eNodeB2, as depicted in Fig. 1. In the proposed system model, we explore a CR scenario in which MTC devices can access the spectrum of the PU as long as the interference generated for the PU, resulting from the MTC device cluster, remains below the PU's tolerable interference limit. In cluster #1, MTC devices generate a fraction $\eta \in (0, 1)$ of the tolerable interference level, while a fraction $(1 - \eta)$ of the tolerable interference is generated by the MTC devices in cluster #2. Therefore, the transmission power of the MTC devices is constrained so that it does not exceed the interference threshold at the PU (Zhang et al., 2013). MTC devices attempt to access the network following a contention-based RA procedure between the MTC devices and the eNB, which consists (as shown in Fig. 2) of the following four steps: (i) preamble transmission; (ii) RA response; (iii) connection request; (iv) connection completion.

Table 1
Comparison between the proposed work and literature references.

| Ref.	Device	Underlay	Overlay	Metric	Clustering	Optimization	Preamble partition
Li et al. (2018)	NB-IoT	✗	✓	Throughput	✗	Throughput	✗
Zhang et al. (2019)	MTC	✗	✗	Throughput, delay	✓	Throughput via choice of back-off parameter	✗ Partition of back-off parameter
Abdullah et al. (2019)	MTC	✗	✓ Sharing cellular BS in TDMA mode	Outage	✓	Outage probability	✗
Our work	MTC	✓	✗	Throughput, delay	✓ Two clusters	Throughput via optimal preamble partition	✓
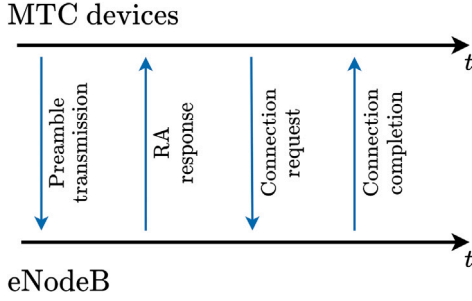
Fig. 2. Contention-based RA procedure of MTC devices accessing the eNB.

Our goal is to investigate the probability of successful access request to an eNB. Whenever an MTC device attempts to access an eNB, it first transmits an access request. In particular, an MTC device selects a preamble of the RACH to transmit an access request according to a slotted Aloha protocol. In contention-based RA, a slotted Aloha protocol can be used with the number of available preambles equal to the number of slots (Li et al., 2015). If two or more devices select the same preamble during the same slot, thus making the eNB unable to decode any preamble, a collision occurs. After the Random Access Response (RAR) for each successfully decoded preamble, the eNB generates an identifier and, then, transmits a RAR to the MTC devices. Next, the MTC device transmits a connection request message with a User Equipment (UE) identifier to the eNB. Eventually, the eNB transmits a connection completion message to the MTC device. If an MTC device does not receive a connection completion message from the eNB, a failure in the contention completion occurs and the MTC device attempts a new access.

3. Performance analysis

In the following, the probability of successful access of an MTC device to the eNB, as a function of its transmit power, is derived. We consider that the allowed PU outage probability at PU is denoted as $\delta \in (0, 1)$. We assume that all the channels are Rayleigh-faded so that the channel power gains are exponentially distributed. The probability of an outage can be expressed as follows:

$$
\begin{aligned}
\mathcal{P}_{\text{pu−out1}} &= \Pr\left\{ P_{\text{TX}_{i,1}^{(\text{pu})}} \mathcal{G}_{i,1}^{(\text{pu})} > \eta I_{\text{th}} \right\} \\
&= 1 - \Pr\left\{ \mathcal{G}_{i,1}^{(\text{pu})} \leq \frac{\eta I_{\text{th}}}{P_{\text{TX}_{i,1}^{(\text{pu})}}} \right\}
\end{aligned}
\tag{1}
$$

where: $P_{\text{TX}_{i,1}^{(\text{pu})}}$ is the transmit power (dimension: [mW]) of the ith MTC device from cluster #1 to PU; $\mathcal{G}_{i,1}^{(\text{pu})}$ is the channel gain (adimensional), exponentially distributed with mean μ_1, from the ith device of cluster #1 to PU; η is the reserved fraction (adimensional) of I_{th}, where I_{th}

is the tolerable interference threshold power (dimension: [mW]). The probability of outage is bounded as follows:

$$
\mathcal{P}_{\text{pu−out1}} \leq \delta.
\tag{2}
$$

Taking into account the exponential distribution of $\mathcal{G}_{i,1}^{(\text{pu})}$, it follows that:

$$
\begin{aligned}
1 - \mathcal{P}_{\text{pu−out1}} &= \Pr\left\{ \mathcal{G}_{i,1}^{(\text{pu})} \leq \frac{\eta I_{\text{th}}}{P_{\text{TX}_{i,1}^{(\text{pu})}}} \right\} \\
&= 1 - e^{-\eta I_{\text{th}}/\mu_1 P_{\text{TX}_{i,1}^{(\text{pu})}}}.
\end{aligned}
\tag{3}
$$

Using (2) in (3), one obtains

$$
e^{-\eta I_{\text{th}}/\mu_1 P_{\text{TX}_{i,1}^{(\text{pu})}}} \leq \delta
\tag{4}
$$

and, then,

$$
\begin{aligned}
&\frac{\eta I_{\text{th}}}{\mu_1 P_{\text{TX}_{i,1}^{(\text{pu})}}} \geq -\log(\delta), \\
&\frac{\eta I_{\text{th}}}{\mu_1 P_{\text{TX}_{i,1}^{(\text{pu})}}} \geq \log\left(\frac{1}{\delta}\right), \\
&P_{\text{TX}_{i,1}^{(\text{pu})}} \leq \frac{\eta I_{\text{th}}}{\mu_1 \log\left(\frac{1}{\delta}\right)}, \\
&P_{\text{TX}_{i,1}^{(\text{pu})}} \leq \frac{-\eta I_{\text{th}}}{\mu_1 \log(\delta)}.
\end{aligned}
\tag{5}
$$

Similarly, the outage probability in cluster #2 can be expressed as

$$
\mathcal{P}_{\text{pu−out2}} = \Pr\left\{ P_{\text{TX}_{i,2}^{(\text{pu})}} \mathcal{G}_{i,2}^{(\text{pu})} > (1 - \eta) I_{\text{th}} \right\}
\tag{6}
$$

where $\mathcal{G}_{i,2}^{(\text{pu})}$ is the channel gain (exponentially distributed with mean equal to μ_2) from the ith device in cluster #2 to the PU. Imposing that $\mathcal{P}_{\text{pu−out2}} \leq \delta$ and carrying out the same analytical steps above, it follows that:

$$
P_{\text{TX}_{i,2}^{(\text{pu})}} \leq \frac{(\eta - 1) I_{\text{th}}}{\mu_2 \log(\delta)}.
\tag{7}
$$

Therefore, the maximum transmit powers of any MTC devices in the two clusters are the ones specified at the right-hand sides of (5) and (7).

The decoding probability of the ith MTC device ($i \in \{1, 2, \ldots, N_1\}$) in cluster #1 at eNodeB1 can be expressed as follows (Oh and Shin, 2017):

$$
\mathcal{P}_{\text{dec}_{i,1}^{(\text{e1})}} = \Pr\left\{ \frac{P_{\text{TX}_{i,1}^{(\text{e1})}} \mathcal{G}_{i,1}^{(\text{e1})}}{P_{\text{TX}_{(\text{pu})}} \mathcal{G}_{(\text{pu})}^{(\text{e1})} + P_{\text{TX}_{i,2}^{(\text{e1})}} \mathcal{G}_{i,2}^{(\text{e1})} + n_0} > \gamma_1 \right\}
\tag{8}
$$

where: $\mathcal{G}_{i,1}^{(\text{e1})}$ is the channel gain (adimensional and exponentially distributed with mean of $1/\lambda_v$) from the ith MTC device of cluster #1 to eNodeB1; $P_{\text{TX}_{(\text{pu})}}$ is the PU transmit power (dimension: [mW]); $\mathcal{G}_{i,2}^{(\text{e1})}$ is the channel gain (adimensional and exponentially distributed with mean of $1/\lambda_x$) from the ith device of cluster #2 to eNodeB1; $\mathcal{G}_{(\text{pu})}^{(\text{e1})}$ is the

channel gain (adimensional and exponentially distributed with mean of $1/\lambda_y$) from PU to eNodeB1; $P_{\text{TX}_{i,1}^{(e1)}}$ is the transmit power (dimension: [mW]) from the ith device in cluster #1 to eNodeB1; $P_{\text{TX}_{i,2}^{(e1)}}$ is the transmit power (dimension: [mW]) from the ith device in cluster #2 to eNodeB1; γ_1 is the threshold (adimensional) above which an MTC device in cluster #1 is decodable at eNodeB1; and n_0 is the thermal noise power (dimension: [mW]), which can be neglected in the scenario of interest.

Let $V = aX + bY$, where $a \triangleq P_{\text{TX}_{i,2}^{(e1)}}$, $b \triangleq P_{\text{TX}_{(pu)}}$, $X \triangleq \mathcal{G}_{i,2}^{(e1)}$, $Y \triangleq \mathcal{G}_{(pu)}^{(e1)}$, $U \triangleq \mathcal{G}_{i,1}^{(e1)}$. From (8), one can write:

$$
\begin{aligned}
\mathcal{P}_{\text{dec}_{i,1}^{(e1)}} &= \Pr\left\{ \frac{U}{V} > \frac{\gamma_1}{P_{\text{TX}_{i,1}^{(pu)}}} \right\} \\
&= \Pr\left\{ W > \alpha_1 \right\} \\
&= 1 - F_W(\alpha_1)
\end{aligned}
\tag{9}
$$

where $W = U/V$ and $\alpha_1 = \gamma_1 / P_{\text{TX}_{i,1}^{(pu)}}$.

In order to evaluate $\mathcal{P}_{\text{dec}_{i,1}^{(e1)}}$, the Probability Density Function (PDF) of $V = aX + bY$ can be expressed as

$$
f_V(v) = \frac{\lambda_x \lambda_y}{\lambda_y a - \lambda_x b}\left(e^{-\lambda_x \frac{v}{a}} - e^{-\lambda_y \frac{v}{b}} \right).
\tag{10}
$$

The corresponding Cumulative Distribution Function (CDF) of $F_W(\alpha_1)$ in (9) can then be written as

$$
\begin{aligned}
F_W(\alpha_1) &= \Pr\left\{ \frac{U}{V} < \alpha_1 \right\} \\
&= \int_0^\infty F_U(\alpha_1 v) f_V(v) dv \\
&= 1 - \frac{\lambda_x \lambda_y}{ab\left(\frac{\lambda_x}{a} + \alpha_1 \lambda_v\right)\left(\frac{\lambda_y}{b} + \alpha_1 \lambda_v\right)}.
\end{aligned}
\tag{11}
$$

Finally, one obtains (see Appendix for details)

$$
\begin{aligned}
\mathcal{P}_{\text{dec}_{i,1}^{(e1)}} &= 1 - F_W(\alpha_1) \\
&= \frac{\lambda_x \lambda_y}{ab\left(\frac{\lambda_x}{a} + \alpha_1 \lambda_v\right)\left(\frac{\lambda_y}{b} + \alpha_1 \lambda_v\right)}.
\end{aligned}
\tag{12}
$$

Similarly, the decoding probability of the ith MTC device ($i \in \{1, 2, \ldots, N_2\}$) in cluster #2 at eNodeB2 can be expressed as:

$$
\begin{aligned}
\mathcal{P}_{\text{dec}_{i,2}^{(e2)}} &= \Pr\left\{ \frac{P_{\text{TX}_{i,2}^{(e2)}} \mathcal{G}_{i,2}^{(e2)}}{P_{\text{TX}_{(pu)}} \mathcal{G}_{(pu)}^{(e2)} + P_{\text{TX}_{i,1}^{(e2)}} \mathcal{G}_{i,1}^{(e2)} + n_0} > \gamma_2 \right\} \\
&= \frac{\lambda_x' \lambda_y'}{a_1 b_1 \left(\frac{\lambda_x'}{a_1} + \alpha_2 \lambda_v'\right)\left(\frac{\lambda_y'}{b_1} + \alpha_2 \lambda_v'\right)}
\end{aligned}
\tag{13}
$$

where: $\alpha_2 \triangleq \gamma_2 / P_{\text{TX}_{i,2}^{(e2)}}$; $a_1 \triangleq P_{\text{TX}_{i,2}^{(e2)}}$; $b_1 \triangleq P_{\text{TX}_{(pu)}}$; $\mathcal{G}_{i,2}^{(e2)}$ is the channel gain from the ith MTC device in cluster #2 to eNodeB2, which is exponentially distributed with mean of $1/\lambda_v'$; $\mathcal{G}_{i,1}^{(e2)}$ is the channel gain from the ith MTC device of cluster #1 to eNodeB2, which is exponentially distributed with mean $1/\lambda_x'$; $\mathcal{G}_{(pu)}^{(e2)}$ is channel gain from PU to eNodeB2, which is exponentially distributed with mean $1/\lambda_y'$; $P_{\text{TX}_{i,1}^{(e2)}}$ is the transmit power from the ith MTC device in cluster #1 to eNodeB2; γ_2 is the threshold above which an MTC device in cluster #2 is decodable at eNodeB2.

3.1. Dynamic adjustment of preamble partition

After clustering the attempting devices into two groups, the eNB dynamically determines the RA preamble partition between the clusters

before letting the MTC devices access the network. In a certain RA slot, we denote: N_1 as the number of MTC devices in cluster #1; N_2 as the number of MTC devices in cluster #2; N_{tot} as the total number of the MTC devices, i.e., $N_{\text{tot}} = N_1 + N_2$. We define the preamble partition β as follows (Li et al., 2015):

$$
\beta \triangleq \frac{M_1}{M_2}
\tag{14}
$$

$$
M_1 + M_2 = M_{\text{tot}}
\tag{15}
$$

where: M_1 represents the number of preambles allocated for cluster #1; M_2 represents the number of preambles allocated for cluster #2; and M_{tot} is the total number of preambles (Li et al., 2015). From (14) and (15), it follows that:

$$
M_1 = \frac{M_{\text{tot}} \beta}{1 + \beta}
\tag{16}
$$

$$
M_2 = \frac{M_{\text{tot}}}{1 + \beta}.
\tag{17}
$$

Since every MTC device selects the preamble randomly from the available pool, collisions may occur if more than one MTC device selects the same preamble (Laya et al., 2013). Moreover, according to the contention-based RA procedure, slotted Aloha is the adopted multiple access protocol, with the number of available preambles equal to the number of slots (Li et al., 2015). In this way, the access success probability can be expressed as (Li et al., 2015)

$$
P_s = e^{-\frac{N}{M}}
\tag{18}
$$

where N is the number of devices and M is the number of preambles available within a RA slot. The average number of devices successfully completing the access attempts from the two clusters can be expressed as follows (Li et al., 2015):

$$
N_{\text{ssa},1} = N_1 f_1 e^{-\frac{N_1 f_1}{M_1}}
\tag{19}
$$

$$
N_{\text{ssa},2} = N_2 f_2 e^{-\frac{N_2 f_2}{M_2}}
\tag{20}
$$

where: f_1 is the ACB factor of cluster #1; and f_2 is the ACB factor of cluster #2.

At this point, we can express the throughput of a device from cluster #1, the throughput of a device from cluster #2, and the total throughput as follows, respectively (Lee et al., 2011; Li et al., 2015):

$$
\mathcal{T}_1 = N_{\text{ssa},1} \mathcal{P}_{\text{dec}_{i,1}^{(e1)}}
\tag{21}
$$

$$
\mathcal{T}_2 = N_{\text{ssa},2} \mathcal{P}_{\text{dec}_{i,2}^{(e2)}}
\tag{22}
$$

$$
\mathcal{T}_{\text{tot}} = \mathcal{T}_1 + \mathcal{T}_2.
\tag{23}
$$

Finally using (12), (13), (19)–(23), we can write:

$$
\begin{aligned}
\mathcal{T}_{\text{tot}} &= \mathcal{P}_{\text{dec}_{i,1}^{(e1)}} N_1 f_1 \exp\left\{ \frac{-N_1 f_1 (1 + \beta)}{M_{\text{tot}} \beta} \right\} \\
&\quad + \mathcal{P}_{\text{dec}_{i,2}^{(e2)}} N_2 f_2 \exp\left\{ \frac{-N_2 f_2 (1 + \beta)}{M_{\text{tot}}} \right\}.
\end{aligned}
\tag{24}
$$

At this point, our goal is to find the optimal value of β which maximizes $\mathcal{T}_{\text{tot}}$. Imposing $\partial \mathcal{T}_{\text{tot}} / \partial \beta = 0$, where

$$
\begin{aligned}
\frac{\partial \mathcal{T}_{\text{tot}}}{\partial \beta} &= \mathcal{P}_{\text{dec}_{i,1}^{(e1)}} N_1 f_1 \exp\left\{ \frac{-N_1 f_1}{M_{\text{tot}}} \right\} \\
&\quad \exp\left\{ \frac{-N_1 f_1}{M_{\text{tot}} \beta} \right\} \left(\frac{N_1 f_1}{M_{\text{tot}} \beta^2} \right) + \mathcal{P}_{\text{dec}_{i,2}^{(e2)}} N_2 f_2 \\
&\quad \exp\left\{ \frac{-N_2 f_2}{M_{\text{tot}}} \right\} \exp\left\{ \frac{-N_2 f_2 \beta}{M_{\text{tot}}} \right\} \left(\frac{-N_2 f_2}{M_{\text{tot}}} \right)
\end{aligned}
\tag{25}
$$

it follows:

$$
\begin{aligned}
&\mathcal{P}_{\text{dec}_{i,1}^{(e1)}} N_1^2 f_1^2 \exp\left\{ \frac{-N_1 f_1}{M_{\text{tot}} \beta} (1 + \beta) \right\} \left(\frac{1}{\beta^2} \right) \\
&= \mathcal{P}_{\text{dec}_{i,2}^{(e2)}} N_2^2 f_2^2 \exp\left\{ \frac{-N_2 f_2}{M_{\text{tot}}} (1 + \beta) \right\}.
\end{aligned}
\tag{26}
$$

Considering the logarithm of both sides of (26), one obtains:

$$\log\left(\mathcal{P}_{\text{dec}_{i,1}}^{(e1)}\right) + 2\log(N_1) + 2\log(f_1) - \left\{\frac{N_1 f_1}{M_{\text{tot}}\beta}(1+\beta)\right\} + \log\left(\frac{1}{\beta^2}\right)$$
$$= \log\left(\mathcal{P}_{\text{dec}_{i,2}}^{(e2)}\right) + 2\log(N_2) + 2\log(f_2) - \left\{\frac{N_2 f_2}{M_{\text{tot}}}(1+\beta)\right\} \quad (27)$$

and, finally,

$$\log\left(\frac{\mathcal{P}_{\text{dec}_{i,1}}^{(e1)}}{\mathcal{P}_{\text{dec}_{i,2}}^{(e2)}}\right) + 2\log\left(\frac{N_1}{N_2}\right) + 2\log\left(\frac{f_1}{f_2}\right)$$
$$= \left\{\frac{N_1 f_1}{M_{\text{tot}}\beta}(1+\beta)\right\} - \left\{\frac{N_2 f_2}{M_{\text{tot}}}(1+\beta)\right\} - \log\left(\frac{1}{\beta^2}\right). \quad (28)$$

The optimal value of β which maximizes the throughput is obtained by solving (28). Since a closed-form expression of the optimal value of β is not available, we obtain such a value by solving the transcendental equation (28) numerically. The highest throughput[1] is obtained by inserting the obtained value of β in (24).

3.2. Delay analysis of M2M communications

We now investigate the system performance in terms of delay. MTC devices transmit RA requests to the eNB with a period of duration T_s. If more than one MTC device sends requests to the eNB using the same preamble at the same time, then RA requests collide and the eNB cannot decode any RA attempt. Whenever a collision occurs, contention is not considered to be resolved. MTC devices can identify the contention resolution results at the last step of the RA. If contention is resolved, then MTC devices will get into RRC connected mode to transmit the data to the eNB. MTC devices repeat the process of transmitting the preambles when contention is not resolved. In this case, devices wait for a specific period of time, denoted as *back-off interval* (ranging from 0 ms to 960 ms Tyagi et al., 2012; Althumali et al., 2020), before retransmitting to the eNB. For simplicity, we consider a back-off interval equal to 0 ms, i.e., no back-off (Tyagi et al., 2012). If more than one MTC device selects the same preamble at the same time, then they re-transmit in the next time. In our system model, we assume that (i) MTC devices re-transmitting the preambles randomly choose a preamble from the available M_{tot} preambles and (ii) choosing the same preamble again is allowed. Denoting the preamble transmission success probability as f, the probability of c collisions before a success can be written as (Tyagi et al., 2012)

$$\text{Pr}\{c \text{ consecutive collisions}\} = (1-f)^c f\left(1 - \mathcal{P}_{\text{dec}_{i,1}}^{(e1)}\right) \quad (29)$$

under the assumption of c independent unsuccessful consecutive transmissions, each with probability $(1-f)$, followed by a successful transmission, with probability f, at the $(c+1)$th attempt.

The probability of an MTC device to experience $c \in \{0, 1, \dots, W-1\}$ collisions can be expressed as follows:

$$\text{Pr}\{\text{MTC device to experience } c \text{ consecutive collisions}\} =$$
$$= \frac{\text{Pr}\{c \text{ consecutive collisions}\}}{\sum_{k=0}^{W-1} \text{Pr}\{k \text{ consecutive collisions}\}}$$
$$= \frac{(1-f)^c f}{\sum_{k=0}^{W-1}(1-f)^k f}\left(1 - \mathcal{P}_{\text{dec}_{i,1}}^{(e1)}\right) \quad (30)$$

where W is the maximum number of allowed retransmissions. The expected number of collisions $\mathbb{E}(C)$ is (Tyagi et al., 2012)

$$\mathbb{E}(C) = \sum_{j=0}^{W-1} j\frac{(1-f)^j f}{\sum_{k=0}^{W-1}(1-f)^k f}\left(1 - \mathcal{P}_{\text{dec}_{i,1}}^{(e1)}\right). \quad (31)$$

Indicating as T_s the duration of a transmission act, the expected delay $\mathbb{E}(D_1)$ can be written as follows:

$$\mathbb{E}(D_1) = T_s \sum_{j=0}^{W-1} j\frac{(1-f)^j f}{\sum_{k=0}^{W-1}(1-f)^k f}\left(1 - \mathcal{P}_{\text{dec}_{i,1}}^{(e1)}\right). \quad (32)$$

In order to account for the delay in the absence of collisions, according to 3GPP (2011) we add $T_s/2$, which is the expected value for a uniform delay in $[0, T_s]$ (Tyagi et al., 2012). Thus, the expected delay in (32) can be expressed as follows:

$$\mathbb{E}(D_1) = \frac{T_s}{2} + T_s \sum_{j=0}^{W-1} j\frac{(1-f)^j f}{\sum_{k=0}^{W-1}(1-f)^k f}\left(1 - \mathcal{P}_{\text{dec}_{i,1}}^{(e1)}\right) \quad (33)$$

$$= \frac{T_s}{2} + \frac{T_s}{\sum_{k=0}^{W-1}(1-f)^k}\sum_{j=0}^{W-1} j(1-f)^j\left(1 - \mathcal{P}_{\text{dec}_{i,1}}^{(e1)}\right). \quad (34)$$

Assuming $\ell < 1$, it holds that

$$\sum_{k=0}^{W-1} \ell^k = \frac{1 - \ell^W}{1 - \ell} \quad (35)$$

and

$$\sum_{k=0}^{W-1} k\ell^k = \ell\frac{1 + (W-1)\ell^W - W\ell^{W-1}}{(1-\ell)^2}. \quad (36)$$

Using (34) and denoting $\gamma \triangleq 1 - f$, the average delay for an MTC device in cluster #1 can be expressed as follows:

$$\mathbb{E}(D_1) = \frac{T_s}{2} + \frac{T_s\gamma(1 + (W-1)\gamma^W - W\gamma^{W-1})}{(1-\gamma)(1-\gamma^W)}\left(1 - \mathcal{P}_{\text{dec}_{i,1}}^{(e1)}\right). \quad (37)$$

Similarly, the average delay for an MTC device in cluster #2 becomes

$$\mathbb{E}(D_2) = \frac{T_s}{2} + \frac{T_s\gamma(1 + (W-1)\gamma^W - W\gamma^{W-1})}{(1-\gamma)(1-\gamma^W)}\left(1 - \mathcal{P}_{\text{dec}_{i,2}}^{(e2)}\right). \quad (38)$$

Using expressions (12) and (13) for $\mathcal{P}_{\text{dec}_{i,1}}^{(e1)}$ and $\mathcal{P}_{\text{dec}_{i,2}}^{(e2)}$ in (37) and (38), respectively, one obtains the following final expressions of the average delays:

$$\mathbb{E}(D_1) = \frac{T_s}{2} + \frac{T_s\gamma(1 + (W-1)\gamma^W - W\gamma^{W-1})}{(1-\gamma)(1-\gamma^W)}$$
$$\cdot \left(1 - \frac{\lambda_x \lambda_y}{ab\left(\frac{\lambda_x}{a} + \alpha_1\lambda_v\right)\left(\frac{\lambda_y}{b} + \alpha_1\lambda_v\right)}\right) \quad (39)$$

$$\mathbb{E}(D_2) = \frac{T_s}{2} + \frac{T_s\gamma(1 + (W-1)\gamma^W - W\gamma^{W-1})}{(1-\gamma)(1-\gamma^W)}$$
$$\cdot \left(1 - \frac{\lambda'_x \lambda'_y}{a_1 b_1\left(\frac{\lambda'_x}{a_1} + \alpha_2\lambda'_v\right)\left(\frac{\lambda'_y}{b_1} + \alpha_2\lambda'_v\right)}\right). \quad (40)$$

4. Results

For the sake of completeness, Table 2 summarizes the notation adopted in the analytical formulation at a glance, as well as the specific values chosen for the involved parameters in the experimental evaluation. In Fig. 3, the throughput is shown as a function of the interference threshold I_{th}. The number of preambles allocated for cluster #1 (namely, M_1) is larger than the number of preambles allocated for cluster #2 (namely, M_2). The throughput performance at eNodeB1 (denoted as $\mathcal{T}_1$) is better than that at eNodeB2 (denoted as $\mathcal{T}_2$). As the interference threshold increases, the throughput of both eNBs increases. A higher value of the interference threshold leads to an increase of the transmit power of the devices, which, in turn, increases the decoding probability and the throughput.

In Fig. 4, the decoding probability is shown as a function of the interference threshold I_{th}. As the value of η is higher in cluster #1 than

---

[1] Considering the throughput expression in (24) it can be verified that $\mathcal{T}_{\text{tot}}$ is monotonically increasing for β between 0 and the value which solves (28), whereas it is monotonically decreasing for larger values. Hence, the value of β which solves (28) is indeed the maximizer of the throughput.

Table 2
Notation adopted in the analytical formulation at a glance, and consequent values chosen for those parameters for the experimental evaluation.

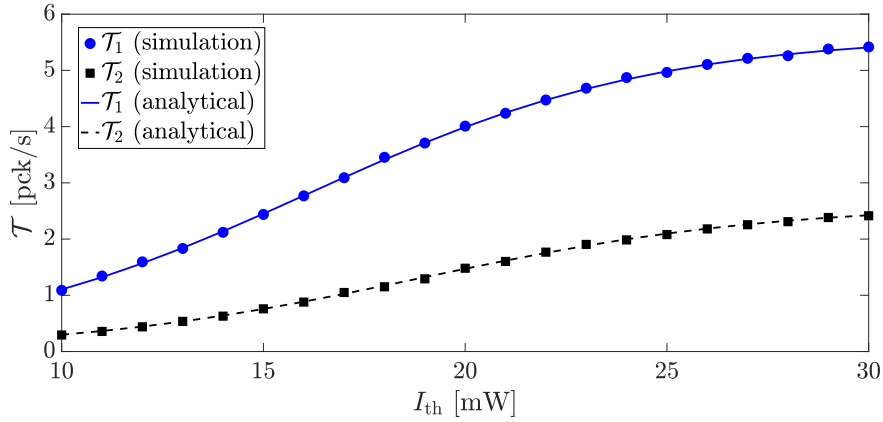| Parameters	Value	Description
$\mu_1, \mu_2, \lambda_v, \lambda_x, \lambda_y, \lambda_v', \lambda_y', \lambda_x'$	1	Mean of $\mathcal{G}_{i,1}^{(pu)}, \mathcal{G}_{i,2}^{(pu)}, \mathcal{G}_{i,2}^{(e2)}, \mathcal{G}_{i,2}^{(e1)}, \mathcal{G}_{(pu)}^{(e1)}, \mathcal{G}_{i,2}^{(e2)}, \mathcal{G}_{(pu)}^{(e2)}, \mathcal{G}_{i,1}^{(e2)}$, respectively (Zhang et al., 2013)
$P_{TX_{(pu)}}$	5 W	PU's transmit power
N_1	60	Number of devices in cluster #1
N_2	50	Number of devices in cluster #2
M_1	30	Number of preambles allocated for cluster #1 (Vardakas et al., 2015)
M_2	24	Number of preambles allocated for cluster #2 (Vardakas et al., 2015)
f_1	0.7	ACB factor of cluster #1 (Tello-Oquendo et al., 2017)
f_2	0.5	ACB factor of cluster #2 (Tello-Oquendo et al., 2017)
γ_1	1 dB	SINR threshold for cluster #1
γ_2	2 dB	SINR threshold for cluster #2
η	0.6	Fraction of I_{th}
δ	0.01	PU outage constraint

Fig. 3. Throughput as a function of the interference threshold I_{th}.
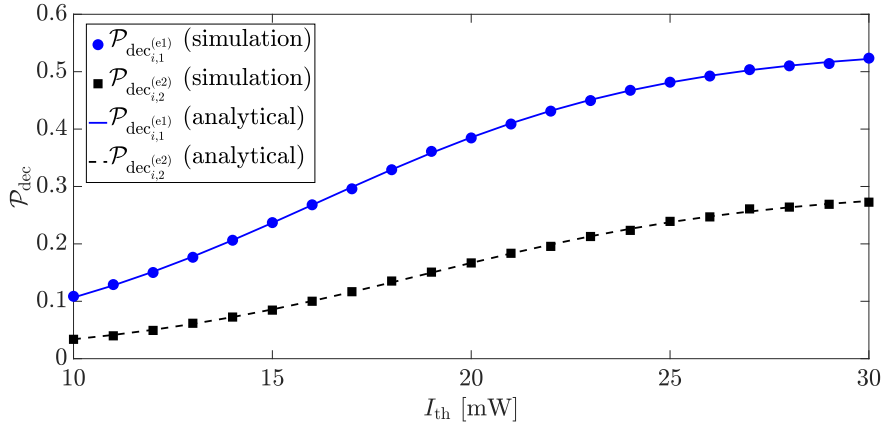

Fig. 4. Decoding probability $\mathcal{P}_{dec}$ as a function of the interference threshold I_{th}.

in cluster #2, the decoding probability of an MTC device in cluster #1 is higher than that of an MTC device in cluster #2. If we increases the tolerable interference threshold level at PU, the decoding probability increases at the eNB (in both cluster #1 and cluster #2).

In Fig. 5, the throughput at the eNB (for both cluster #1 and cluster #2) is shown as a function of the interference threshold for various values of the ACB factor. It can be observed that the throughput is higher at both eNBs when the ACB factor is 0.5. For higher values of the ACB factor, the throughput reduces. As the ACB factor increases, the traffic intensity increases because of a larger number of access attempts. Because of this, there is a higher chance that two or more devices select

the same preamble during the same slot so that the eNB is unable to decode any preamble: therefore, a larger number of collisions occurs and the throughput at the eNB reduces.

In Fig. 6, the throughput is shown as a function of the interference threshold, for various values of the outage constraint. The throughput is higher for higher outage constraint, as higher values of the outage constraint allow the transmit power of the devices to increase. The results in Table 3 highlight that the throughput is maximized in correspondence to the optimal value of the preamble partition β (which solves (28)) that depends on the values of N_1 and N_2.
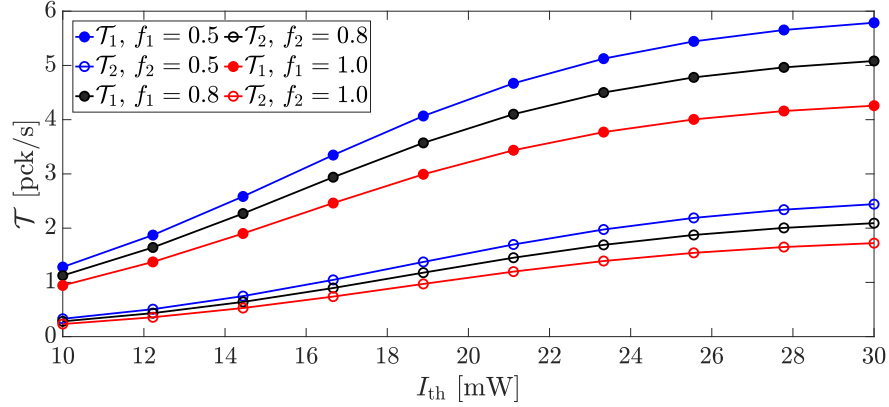
Fig. 5. Throughput as a function of the interference threshold I_{th} for various values of the ACB factor f.
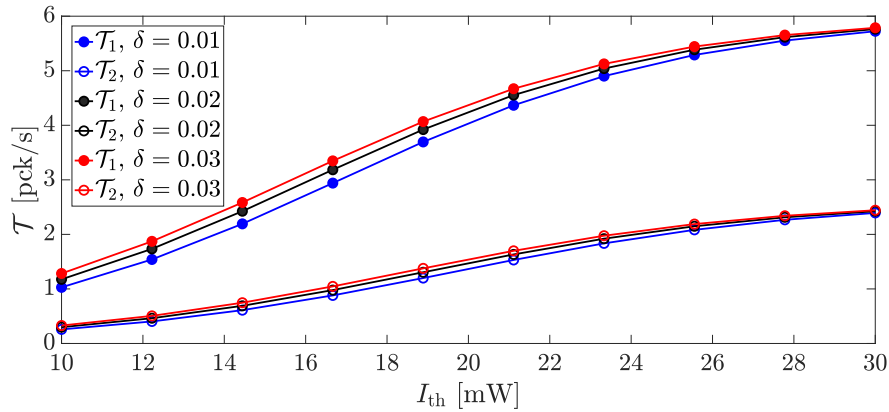

Fig. 6. Throughput as a function of the interference threshold I_{th} for various values of the outage constraint δ.

Table 3
Optimal value of the preamble partition β for various values of N_1, N_2, M_1, and M_2.

N_1	N_2	M_1	M_2	β
10	50	18	36	0.48
20	40	30	24	1.21
30	60	32	22	1.45
50	50	40	14	2.85

In Fig. 7, the throughput is shown as a function of the preamble partition β. As the number of preambles allocated for cluster #1 increases, the throughput at eNodeB1 increases. Since the total number of preambles is fixed, the number of preambles allocated for cluster #2 reduces, so that the throughput at eNodeB2 decreases. Even in this case, it can be observed that the total throughput is maximized in correspondence to a specific value of β.

In Fig. 8, the average delay is shown as a function of the number of devices, for various values of preambles, while keeping the interference threshold identical for both clusters of devices. Therefore, as the number of devices increases, the average delay increases because the collision rate increases. However, if we compare the average delay of clusters with different preambles, then the cluster which has the larger number of preambles has a lower average delay, if compared to the other cluster which has a smaller number of preambles. Intuitively, increasing the number of preambles reduces the probability of collision and, then, the average delay.

In Fig. 9, the average delay is shown as a function of the number of devices for various values of the interference threshold. The cluster with higher interference threshold leads to an increase of the transmit power of the devices, which increases the decoding probability. Therefore, increasing the interference threshold reduces the average delay.

In Fig. 10, the average delay is shown as a function of the number of devices for various values of maximum number of times (W) a request is made to the eNB. The average delay is higher for the cluster with higher value of W. When the number of request attempts increases, then the collision rate increases as well. If the RA mechanism fails after a collision, then the device must wait for some time before starting a new RA: this introduces a latency in accessing the channel, thus increasing the average delay.

In Fig. 11, the optimal value of the preamble partition β is shown as a function of the tolerable interference threshold (I_{th}). The decoding probability is an increasing function of I_{th}, as the transmit powers of MTC devices increase (as shown in Fig. 4). The optimal value of β, which maximizes the throughput, reduces for increasing value of I_{th}. Due to the choice of a higher value of η in cluster #1, the decoding probability is higher in cluster #1, which allows more preambles to be assigned to cluster #1.

5. Conclusions

In this paper, we have investigated the design of CR MTC networks. The throughput and delay performance of two clusters of MTC devices has been investigated in an underlay CR network. A higher value of tolerable interference threshold of a primary network increases the preambles' decoding probability and the throughput, while it reduces the delay. An optimal value of the preamble partition β allows to
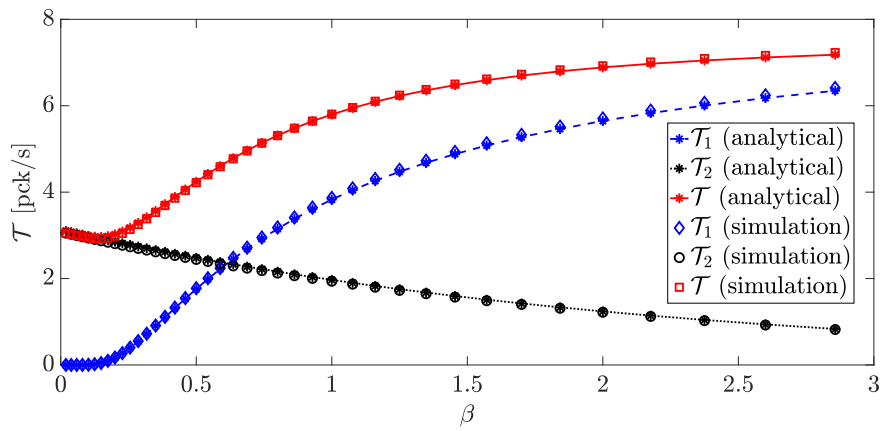
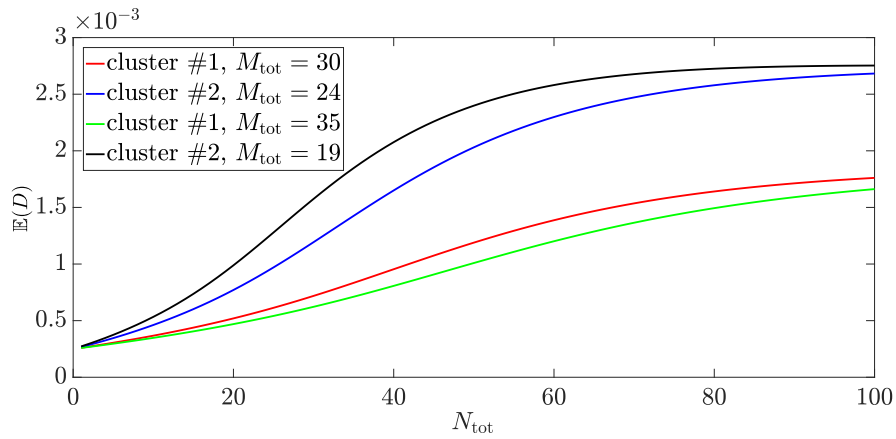**Fig. 7.** Throughput as a function of the preamble partition β.

Fig. 8. Average delay $\mathbb{E}(D)$ as a function of the number of MTC devices N_{tot}, for various values of the number of preambles M_{tot}.
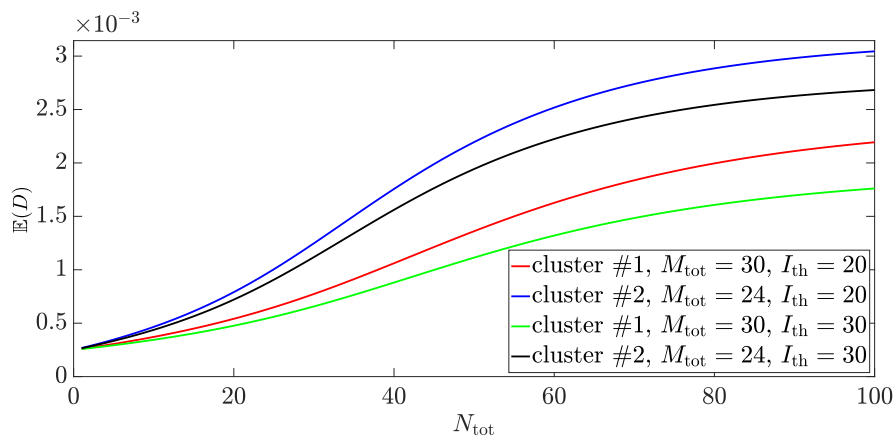

Fig. 9. Average delay $\mathbb{E}(D)$ as a function of the number of MTC devices N_{tot} with different interference thresholds I_{th}.
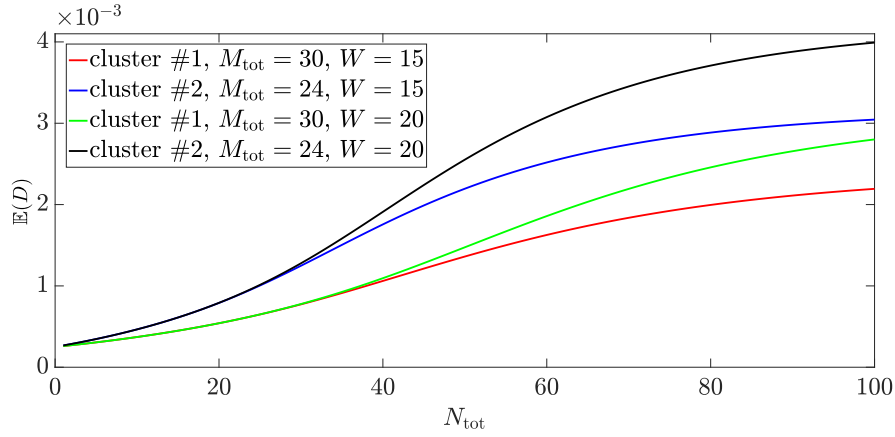
Fig. 10. Average delay $\mathbb{E}(D)$ as a function of the number of MTC devices N_{tot} with different number of requests W made to an eNB.
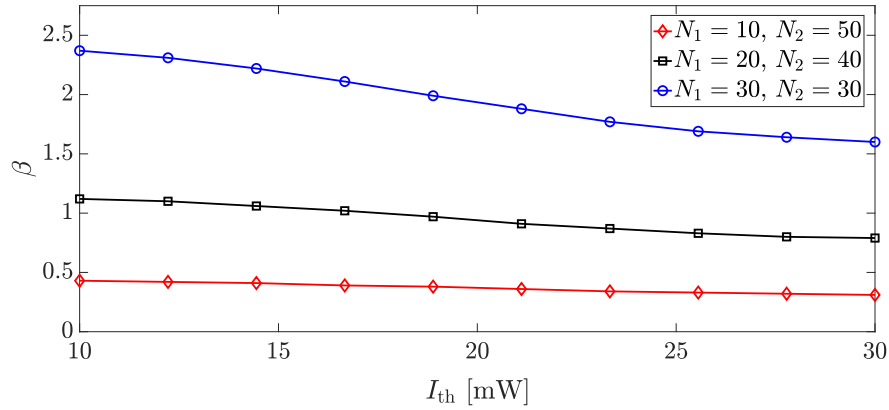

Fig. 11. Optimal value of the preamble partition β as a function of the interference threshold I_{th}.

maximize the throughput, which also depends on the ACB factor, the number of MTC devices in each cluster, as well as the interference threshold via decoding probability. A higher value of the ACB factor reduces the throughput. The average delay is an increasing function of the number of preambles and re-transmission attempts.

CRediT authorship contribution statement

Soumen Mondal: Conceptualization, Data curation, Formal analysis, Investigation, Methodology, Resources, Software, Validation, Visualization, Writing – original draft, Writing – review & editing. **Luca Davoli:** Investigation, Methodology, Visualization, Writing – original draft, Writing – review & editing. **Sanjay Dhar Roy:** Conceptualization, Data curation, Formal analysis, Funding acquisition, Investigation, Methodology, Project administration, Resources, Supervision, Validation, Writing – original draft, Writing – review & editing. **Sumit Kundu:** Conceptualization, Data curation, Formal analysis, Funding acquisition, Investigation, Methodology, Project administration, Resources, Supervision, Validation, Visualization, Writing – original draft, Writing – review & editing. **Gianluigi Ferrari:** Conceptualization, Data curation, Formal analysis, Funding acquisition, Investigation, Methodology, Project administration, Resources, Supervision, Validation, Visualization, Writing – original draft, Writing – review & editing. **Riccardo Raheli:** Conceptualization, Data curation, Formal analysis, Funding acquisition, Investigation, Methodology, Project administration, Resources, Supervision, Validation, Visualization, Writing – original draft, Writing – review & editing.

Declaration of competing interest

The authors declare that they have no known competing financial interests or personal relationships that could have appeared to influence the work reported in this paper.

Data availability

The authors are unable or have chosen not to specify which data has been used.

Appendix. Derivation of (11)

The CDF $F_W(\alpha_1)$ can be expressed as follows:

$$
\begin{aligned}
F_W(\alpha_1) &= \Pr\left\{\frac{U}{V} < \alpha_1\right\} \\
&= \Pr\left\{U < \alpha_1 V\right\} \\
&= \int_0^\infty \Pr\left\{U < \alpha_1 v \mid V = v\right\} f_V(v)\, dv \\
&= \int_0^\infty F_U(\alpha_1 v) f_V(v)\, dv \\
&= \int_0^\infty \left(1 - e^{-\lambda_v \alpha_1 v}\right) \frac{\lambda_x \lambda_x}{\lambda_x a - \lambda_x b}\left(e^{-\lambda_x \frac{v}{a}} - e^{-\lambda_x \frac{v}{b}}\right) dv \\
&= 1 - \int_0^\infty \frac{\lambda_x \lambda_x}{\lambda_x a - \lambda_x b}\left(e^{-\lambda_x \frac{v}{a}} - e^{-\lambda_x \frac{v}{b}}\right) e^{-\lambda_v \alpha_1 v}\, dv \\
&= 1 - \frac{\lambda_x \lambda_x}{\lambda_x a - \lambda_x b}\int_0^\infty e^{-\left(\frac{\lambda_x}{a} + \alpha_1 \lambda_v\right)v}\, dv \\
&\quad + \frac{\lambda_x \lambda_x}{\lambda_x a - \lambda_x b}\int_0^\infty e^{-\left(\frac{\lambda_x}{b} + \alpha_1 \lambda_v\right)v}\, dv
\end{aligned}
$$

$$= 1 - \frac{\lambda_x \lambda_x}{\lambda_x a - \lambda_x b} \frac{1}{\frac{\lambda_x}{a} + \alpha_1 \lambda_v} + \frac{\lambda_x \lambda_x}{\lambda_x a - \lambda_x b} \frac{1}{\frac{\lambda_x}{b} + \alpha_1 \lambda_v}$$

$$= 1 - \frac{\lambda_x \lambda_x}{\lambda_x a - \lambda_x b} \left[\frac{1}{\frac{\lambda_x}{a} + \alpha_1 \lambda_v} - \frac{1}{\frac{\lambda_x}{b} + \alpha_1 \lambda_v} \right]$$

$$= 1 - \frac{\lambda_x \lambda_x}{ab \left(\frac{\lambda_x}{a} + \alpha_1 \lambda_v \right) \left(\frac{\lambda_x}{b} + \alpha_1 \lambda_v \right)}.$$

References

3GPP, 2011. RAN Improvements for Machine-type Communications. Technical Specification (TS) 37.868, 3rd Generation Partnership Project (3GPP), URL https://portal.3gpp.org/desktopmodules/Specifications/SpecificationDetails.aspx?specificationId=2630, Version 1.0.0.

Abdullah, M.A., Abdullah, Z., Chen, G., Tang, J., Chambers, J., 2019. Performance analysis of cognitive clustered M2M random networks with joint user and machine device selection. IEEE Access 7, 83515–83525. http://dx.doi.org/10.1109/ACCESS.2019.2924522.

Aijaz, A., Aghvami, A.H., 2015. Cognitive machine-to-machine communications for internet-of-things: A protocol stack perspective. IEEE Internet Things J. 2 (2), 103–112. http://dx.doi.org/10.1109/JIOT.2015.2390775.

Alhussien, N., Gulliver, T.A., 2022. Energy-efficient interference-aware cognitive machine-to-machine communications underlaying cellular networks. IEEE Access 10, 33932–33942. http://dx.doi.org/10.1109/ACCESS.2022.3162252.

Althumali, H.D., Othman, M., Noordin, N.K., Hanapi, Z.M., 2020. Dynamic backoff collision resolution for massive M2M random access in cellular IoT networks. IEEE Access 8, 201345–201359. http://dx.doi.org/10.1109/ACCESS.2020.3036398.

Chowdhury, M.R., De, S., 2022. Queue-aware access prioritization for massive machine-type communication. IEEE Internet Things J. 9 (17), 15858–15873. http://dx.doi.org/10.1109/JIOT.2022.3151408.

Debbabi, F., Jmal, R., Fourati, L.C., Aguiar, R.L., 2022. An overview of interslice and intraslice resource allocation in B5G telecommunication networks. IEEE Trans. Netw. Serv. Manag. 19 (4), 5120–5132. http://dx.doi.org/10.1109/TNSM.2022.3189925.

Di, C., Zhang, B., Liang, Q., Li, S., Guo, Y., 2019. Learning automata-based access class barring scheme for massive random access in machine-to-machine communications. IEEE Internet Things J. 6 (4), 6007–6017. http://dx.doi.org/10.1109/JIOT.2018.2867937.

Ejaz, W., Ibnkahla, M., 2015. Machine-to-machine communications in cognitive cellular systems. In: 2015 IEEE International Conference on Ubiquitous Wireless Broadband. ICUWB, Montreal, QC, Canada, pp. 1–5. http://dx.doi.org/10.1109/ICUWB.2015.7324472.

Guo, Z., Zhu, X., Wei, Z., Jiang, Y., Wang, Y., 2022. Collision-aware random access control with preamble reuse for industrial IoT. In: 2022 IEEE 95th Vehicular Technology Conference:(VTC2022-Spring). IEEE, pp. 1–6. http://dx.doi.org/10.1109/VTC2022-Spring54318.2022.9860484.

Ha, S., Seo, H., Moon, Y., Lee, D., Jeong, J., 2018. A novel solution for NB-IoT cell coverage expansion. In: 2018 Global Internet of Things Summit. GIoTS, Bilbao, Spain, pp. 1–5. http://dx.doi.org/10.1109/GIOTS.2018.8534519.

Jiang, N., Deng, Y., Condoluci, M., Guo, W., Nallanathan, A., Dohler, M., 2018. RACH preamble repetition in NB-IoT network. IEEE Commun. Lett. 22 (6), 1244–1247. http://dx.doi.org/10.1109/LCOMM.2018.2793274.

Laya, A., Alonso, L., Alonso-Zarate, J., 2013. Is the random access channel of LTE and LTE-A suitable for M2M communications? A survey of alternatives. IEEE Commun. Surv. Tutor. 16 (1), 4–16. http://dx.doi.org/10.1109/SURV.2013.111313.00244.

Lee, K.-D., Kim, S., Yi, B., 2011. Throughput comparison of random access methods for M2M service over LTE networks. In: GLOBECOM Workshops (GC Wkshps), 2011 IEEE. Houston, TX, USA, pp. 373–377. http://dx.doi.org/10.1109/GLOCOMW.2011.6162474.

Li, W., Du, Q., Liu, L., Ren, P., Wang, Y., Sun, L., 2015. Dynamic allocation of RACH resource for clustered M2M communications in LTE networks. In: Identification, Information, and Knowledge in the Internet of Things (IIKI), 2015 International Conference on. Beijing, China, pp. 140–145. http://dx.doi.org/10.1109/IIKI.2015.38.

Li, T., Yuan, J., Torlak, M., 2018. Network throughput optimization for random access narrowband cognitive radio Internet of Things (NB-CR-IoT). IEEE Internet Things J. 5 (3), 1436–1448. http://dx.doi.org/10.1109/JIOT.2017.2789217.

Mitola, J., Maguire, G.Q., 1999. Cognitive radio: Making software radios more personal. IEEE Pers. Commun. 6 (4), 13–18. http://dx.doi.org/10.1109/98.788210.

Oh, S.-M., Shin, J., 2017. An efficient small data transmission scheme in the 3GPP NB-IoT system. IEEE Commun. Lett. 21 (3), 660–663. http://dx.doi.org/10.1109/LCOMM.2016.2632128.

Swain, S.N., Subudhi, A., 2023. Recurrent neural network based RACH scheme minimizing collisions in 5G and beyond networks. In: IEEE INFOCOM 2023-IEEE Conference on Computer Communications Workshops. INFOCOM WKSHPS, IEEE, pp. 1–7. http://dx.doi.org/10.1109/INFOCOMWKSHPS57453.2023.10226096.

Tello-Oquendo, L., Leyva-Mayorga, I., Pla, V., Martinez-Bauset, J., Vidal, J.-R., Casares-Giner, V., Guijarro, L., 2017. Performance analysis and optimal access class barring parameter configuration in LTE-A networks with massive M2M traffic. IEEE Trans. Veh. Technol. 67 (4), 3505–3520. http://dx.doi.org/10.1109/TVT.2017.2776868.

Tyagi, R.R., Lee, K.-D., Aurzada, F., Kim, S., Reisslein, M., 2012. Efficient delivery of frequent small data for U-healthcare applications over LTE-advanced networks. In: Proceedings of the 2nd ACM International Workshop on Pervasive Wireless Healthcare. MobileHealth '12, Hilton Head, South Carolina, USA, pp. 27—32. http://dx.doi.org/10.1145/2248341.2248354.

Vardakas, J.S., Zorba, N., Skianis, C., Verikoukis, C.V., 2015. Performance analysis of M2M communication networks for QoS-differentiated smart grid applications. In: 2015 IEEE Globecom Workshops. GC Wkshps, IEEE, pp. 1–6. http://dx.doi.org/10.1109/GLOCOMW.2015.7414116.

Yang, B., Wei, F., She, X., Jiang, Z., Zhu, J., Chen, P., Wang, J., 2023. Intelligent random access for massive-machine type communications in sliced mobile networks. Electronics 12 (2), 329. http://dx.doi.org/10.3390/electronics12020329.

Yao, H., Huang, T., Zhao, C., Kang, X., Liu, Z., 2014. Optimal power allocation in cognitive radio based machine-to-machine network. EURASIP J. Wireless Commun. Networking 2014, 1–9. http://dx.doi.org/10.1186/1687-1499-2014-82.

Zhang, C., Sun, X., Xia, W., Huang, R., Zhou, M., Zhu, H., 2023. Access delay optimization of double-contention random access scheme in machine-to-machine communications. IEEE Commun. Lett. http://dx.doi.org/10.1109/LCOMM.2023.3280920.

Zhang, C., Sun, X., Xia, W., Zhang, J., Zhu, H., Wang, X., 2022. Deep learning based double-contention random access for massive machine-type communication. IEEE Trans. Wireless Commun. 22 (3), 1794–1807. http://dx.doi.org/10.1109/TWC.2022.3206769.

Zhang, C., Sun, X., Zhang, J., Wang, X., Jin, S., Zhu, H., 2019. Throughput optimization with delay guarantee for massive random access of M2M communications in industrial IoT. IEEE Internet Things J. 6 (6), 10077–10092. http://dx.doi.org/10.1109/JIOT.2019.2935548.

Zhang, X., Xing, J., Yan, Z., Gao, Y., Wang, W., 2013. Outage performance study of cognitive relay networks with imperfect channel knowledge. IEEE Commun. Lett. 17 (1), 27–30. http://dx.doi.org/10.1109/LCOMM.2012.112812.121371.

Soumen Mondal received his B.Tech degree in Electronics and Communication Engineering in 2008 from Haldia Institute of Technology, Haldia, India, and M.Tech. degree in Telecommunication Engineering in 2010 from NIT, Durgapur. After that he joined Central Mechanical Engineering Research Institute, Durgapur as a Junior Research Fellow in 2010. After that he joined Bengal College of Engineering and Technology, Durgapur as an Assistant Professor in Electronics and Communication Dept on 2012. He completed his Ph.D. under Visvesvaraya Ph.D. scheme in department of Electronics and Communication Engineering, National Institute of Technology Durgapur in 2021. His research interests include Cognitive Radio Networks, Energy Harvesting, NOMA, MIMO, and FSO. He is serving as reviewer of IEEE Wireless Communication Letter and IEEE Communication Letter.

Luca Davoli is a non-tenured Assistant Professor at the Internet of Things (IoT) Laboratory, Department of Engineering and Architecture, University of Parma, Italy. He obtained his Dr. Ing. degree in Computer Engineering and his Ph.D. in Information Technologies at the Department of Information Engineering of the same university, in 2013 and 2017, respectively. He is an IEEE member. His research interests focus on Internet of Things (IoT), Pervasive Computing, Software-Defined Networking, and smart systems. He has served as Editorial Board Member and Technical Program Committee Member of international journals and conferences.

Sanjay Dhar Roy received his B. E. (Hons.) degree in Electronics & Telecommunication Engineering in 1997 from Jadavpur University, Kolkata, India, and M. Tech. in Telecommunication Engineering in 2008 from NIT Durgapur, and Ph.D. in Wireless Communication in 2011 from NIT Durgapur, respectively. He worked for UshaFone, a mobile communication company, from 1997 to 2000. He joined the Department of Electronics & Communication Engineering, NIT Durgapur as a lecturer in 2000 and is currently an Associate Professor there. He is an IEEE senior member. His research interests include Radio Resource Management, Handoff, Device to Device Communication, Cognitive Radio

Networks, CR Femto Cell Networks, Physical Layer Security and Energy Harvesting in Cognitive Radio Networks, Cooperative Cognitive Relay Networks, Cellular IoT and 5G networks. As of today, he has published more than two hundred (200) research papers in various reputed journals and conferences. He has reviewed for various IEEE journals and different journal papers and books from Elsevier, Springer, and Wiley, etc. He has reviewed for IEEE Globecom, IEEE WCNC, IEEE VTC, IEEE PIMRC, IEEE WIMob and NCC on several occasions.

Sumit Kundu received Bachelor of Engineering (Hons) in Electronics & Communication Engineering from National Institute of Technology, Durgapur (Erstwhile Regional Engg College, Durgapur, University of Burdwan) with University Gold medal in 1991, Master of Technology (M.Tech) in Telecommunication Systems Engineering from IIT Kharagpur in 1993–94 and Ph.D (Wireless Communication) from IIT Kharagpur in 2004. He has been a faculty in the Department of ECE, NIT Durgapur since 1995 where he is currently a Full Time Professor (Higher Administrative Grade). He also served as an Assistant Professor in the G.S.Sanyal School of Telecommunications, IIT Kharagpur for a year in 2007. He has supervised 11 PhDs so far in the domain of Wireless Communication and Networking and continuing supervision for several more students. He has published more than 200 research papers in international journal, national and international conferences, and contributed to several book chapters. His current areas of research includes Cooperative Communication, NOMA for 5G, Intelligent Reflecting Surfaces (IRS), Cognitive Radio Network, Energy Harvesting in Wireless Networks, Physical Layer Security, Wireless Sensor Networks. He is an IEEE

senior member. He is reviewer of several papers for IEEE, Elsevier, Wiley journals, etc., and many important national and international IEEE conferences.

Gianluigi Ferrari received the Laurea (*summa cum laude*) and Ph.D. degrees in Electrical Engineering from the University of Parma, Parma, Italy, in 1998 and 2002, respectively. Since 2002, he has been with the University of Parma, where he is currently a Full Professor of Telecommunications and also the coordinator of the Internet of Things (IoT) Laboratory, Department of Engineering and Architecture. He is co-founder and President of things2i ltd., a spin-off of the University of Parma dedicated to IoT and smart systems. He is an IEEE senior member. His current research interests include signal processing, advanced communication and networking, IoT and smart systems.

Riccardo Raheli is Professor of Communication Engineering at the University of Parma, Italy, which he joined in 1991. From 1988 to 1991, he was with the Sant'Anna School of Advanced Studies, Pisa, Italy. From 1986 to 1988 he was with Siemens Telecommunications, Milan, Italy. In 1990 and 1993, he spent leaves as a Visiting Assistant Professor at the University of Southern California, Los Angeles, USA. His scientific interests are in the general area of systems for communication, processing and storage of information, in which he has published diversely and extensively. He is an IEEE life member. He has served as Editorial Board Member and Technical Program Committee Co-Chair of prestigious international journals and conferences.